Gigahertz Dynamics of a Strongly Driven Single Quantum Spin

G. D. Fuchs,[1] V. V. Dobrovitski,[2] D. M. Toyli,[1] F. J. Heremans,[1] D. D. Awschalom[1]*

Two-level systems are at the core of numerous real-world technologies such as magnetic resonance imaging and atomic clocks. Coherent control of the state is achieved with an oscillating field that drives dynamics at a rate determined by its amplitude. As the strength of the field is increased, a different regime emerges where linear scaling of the manipulation rate breaks down and complex dynamics are expected. By calibrating the spin rotation with an adiabatic passage, we have measured the room-temperature "strong-driving" dynamics of a single nitrogen vacancy center in diamond. With an adiabatic passage to calibrate the spin rotation, we observed dynamics on sub-nanosecond time scales. Contrary to conventional thinking, this breakdown of the rotating wave approximation provides opportunities for time-optimal quantum control of a single spin.

Two-level quantum systems have proven a fruitful ground for many emerging technologies. Recently, there have been a growing number of solid-state implementations of individually addressable two-level systems (*1*) for quantum information processing as well as fundamental studies of a single quantum object. These include superconducting qubits (*2*, *3*), optically and electrically controlled single spins in quantum dots (*4*–*6*), individual charges in quantum dots (*7*), donors in Si (*8*, *9*), and nitrogen vacancy (NV) centers in diamond (*10*–*13*). A critical issue for quantum information processing is the rate at which the two-level state can be manipulated compared to its coherence time because of the practical need for fault-tolerance (*14*). This necessitates efforts to both extend the coherence time and increase the manipulation rate of two-level systems.

Coherent manipulation of two-level systems is commonly achieved by applying a weak oscillating field at a frequency resonant with the energy level splitting (*15*). These driven two-level dynamics are described in terms of a pseudospin-1/2 with a Larmor field, H_0, responding to an oscillating field that is the sum of two fields that rotate in opposite directions. One of the fields rotates with the spin during its precession and applies a constant torque. This corotating field produces Rabi oscillations between the two energy eigenstates because of spin precession around it. The counterrotating field has negligible impact on the spin dynamics provided that it is small compared with H_0 because the direction of the torque it applies on the spin varies rapidly in time and therefore averages out. This argument forms the basis of the rotating wave approximation (*15*) and is the cornerstone of both theory and experiment for nearly all two-level resonance phenomena. In the "strong-driving" regime, where the rotating fields have amplitudes roughly equal to H_0, the spin dynamics are predicted (*16*, *17*) to become highly anharmonic as the co- and counter-rotating fields generate dynamics on the same time scale as the Larmor precession. These dynamics are not chaotic, but they are also not a small modulation of sinusoidal Rabi oscillations seen in classical systems (*18*). We experimentally examined these dynamics in a single quantum spin at room temperature by using an NV center in diamond driven by an oscillating field through an on-chip waveguide. This regime has been of strong theoretical interest on fundamental grounds (*16*, *17*) and in the context of optimal control theory (*19*–*21*). Rather than avoiding the effects of the counterrotating field, we studied its influence on a single spin where the dynamics can be transparently interpreted. We found that it can be exploited to produce sub-nanosecond spin flips. Lastly, to understand these results more deeply, we theoretically modeled our experiment and captured the important details.

An NV center is a spin-1 diamond lattice defect composed of a substitutional nitrogen atom with an adjacent lattice vacancy. In this room-temperature experiment, we operated at a static external field of 850 G so that the energy splitting of the $m_s = 0$ and $m_s = -1$ spin states was 0.49 GHz (Fig. 1A). This splitting is the Larmor field, H_0, given in frequency units because it determines the natural precession rate of the spin. In addition, the $m_s = 0$ to $+1$ transition is strongly Zeeman split from the $m_s = 0$ to -1 transition by ~4.8 GHz, so the NV center dynamics should remain that of a pseudospin-1/2 at the strongest driving field. Spin-selective relaxation from the $m_s = \pm 1$ state via an alternative pathway causes the visible photoluminescence intensity, I_{PL}, to be linearly dependent on the population P of the $m_s = 0$ spin level (*22*, *23*). Because the relaxation end-point is $m_s = 0$, illumination initializes the spin into this state (Fig. 1A). In our time-domain measurements, we first optically initialized the NV center and turned the laser off. A pulsed, microwave-frequency driving field was then applied, and lastly the laser and the photon detector were turned on for readout (Fig. 1B).

The microwave driving field was applied via high-bandwidth, short-terminated coplanar waveguides fabricated on the surface of a [001]-oriented type Ib diamond using optical lithography (Fig. 1, C and D). For weak driving, when we apply a pulse of microwave radiation, P will evolve from the initialized state ($P = 1$) according to Rabi's formula (*15*):

$$P = 1 - \frac{H_1^2}{H_1^2 + \Delta H_0^2} \sin^2\left(\pi \sqrt{H_1^2 + \Delta H_0^2}\, t\right) \quad (1)$$

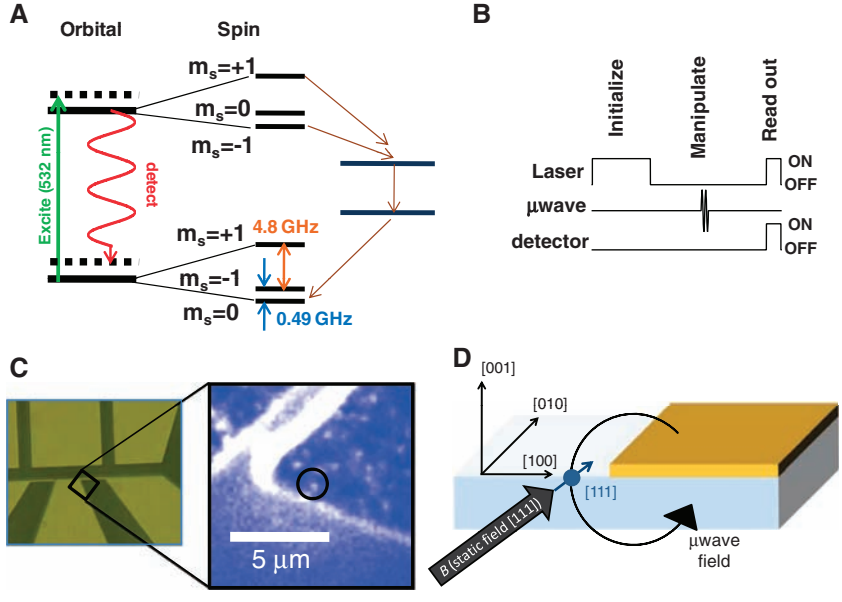

Fig. 1. (**A**) Simplified level structure of an NV center including orbital and spin levels at $B = 850$ G. Spin-selective relaxation from $m_s = \pm 1$ into $m_s = 0$ via an alternative pathway enables read out of the spin state via photoluminescence and optical pumping into the spin ground state. (**B**) Measurement duty cycle. (**C**) (Left) Optical micrograph of the terminated section of the coplanar waveguide on diamond. (Right) Spatial photoluminescence map of the diamond substrate near the waveguide termination. The small white spots are NV centers. The NV center that we describe is circled. (**D**) Experimental geometry.

[1]Center for Spintronics and Quantum Computation, University of California, Santa Barbara, CA 93106, USA. [2]Ames Laboratory and Iowa State University, Ames, IA 50011, USA.

*To whom correspondence should be addressed. E-mail: awsch@physics.ucsb.edu

where ΔH_0 is the detuning from the transition frequency H_0, H_1 is the amplitude of the rotating fields, and t is time. We used microwave pulses resonant with the transition so that $\Delta H_0 \sim 0$. In the experiment, we did not directly monitor the continuous time evolution of P; instead we sampled the evolution by applying microwave pulses of progressively longer duration and then measured P (Fig. 1B). For weak driving, we expected sinusoidal oscillations between I_{PL} for the $m_s = 0$ state ($P = 1$) and I_{PL} for the $m_s = -1$ state ($P = 0$) with an oscillation frequency given by H_1. The I_{PL} values of these eigenstates were calibrated by measuring I_{PL} after optical initialization into $m_s = 0$ and after an adiabatic passage into $m_s = -1$ (*24*). Figure 2A shows a plot of the Rabi frequency measured as a function of microwave power, which follows a square root trend (solid line). Figure 2B shows five Rabi measurements represented by the points in Fig. 2A.

The experimental Rabi oscillations at the smallest driving field, $H_1 = 29$ MHz, are smooth and sinusoidal, in agreement with Eq. 1. As we drove the spin harder, anharmonic components and steps emerged. At 223 MHz, there is an apparent "stalling" of P for a few ranges of pulse widths. Lastly, at $H_1 = 440$ MHz ($H_0/H_1 \sim 1.1$) the driving is strongly nonlinear; at some points, the spin was rotating much faster than expected from the corotating component of driving field alone. In this regime, the co- and counterrotating fields can either act in concert to rapidly change P or act against one another to keep P constant for an extended period. For example at $t \sim 7.5$ ns and $H_1 = 440$ MHz, there is a complete spin flip from pulses whose widths nominally differ by less than 0.5 ns (arrow, Fig. 2B).

To gain more insight into these dynamics, we performed numerical simulations by using pulses measured from the experiment with no free parameters (*24*). Figure 2C shows the simulated time evolution of P during the microwave pulse with a nominal duration of 10 ns, plotted below on the same time axis. The simulation shows dynamics qualitatively similar to those in the experiment, including stalling and periods of fast spin rotation. The simulations also show the population of $m_s = +1$ is at or below 10^{-5} even for the strongest driving field, confirming our assumption that the behavior is purely that of a pseudospin-1/2.

Simulations were performed separately for each experimental pulse to determine the final state populations and account for transient effects in the experiment. Strong-driving pulses are short and intense, so the leading and trailing edges unavoidably make up a substantial fraction of the pulse and have more influence than in standard spin resonance experiments. The simulated final state populations, plotted in Fig. 2D next to the experimental data, are in excellent qualitative

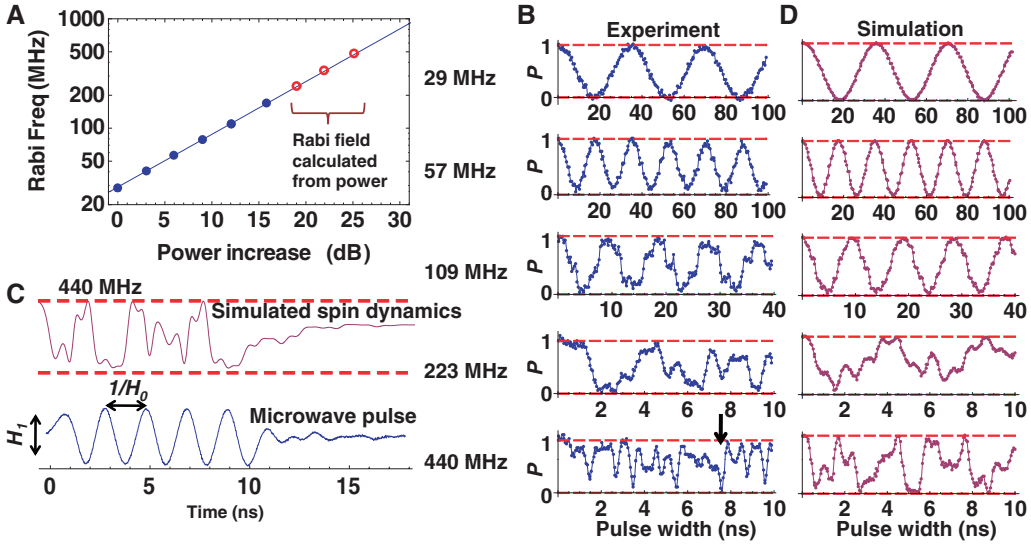

Fig. 2. (**A**) Experimental Rabi frequency as a function of microwave power at a static magnetic field of 850 G applied along the NV symmetry axis (H_0 for the $m_s = 0$ to -1 transition is 0.49 GHz). The Rabi field is calculated from the power for the open circles because the data do not fit to a sinusoid. (**B**) Experimental Rabi oscillations measured by collecting I_{PL} as a function of pulse width for five different driving fields, H_1. The dashed red lines correspond to an $m_s = 0$ population P of 1 (upper) and 0 (lower). (**C**) P as a function of time for simulated spin dynamics using the microwave pulse from the experiment. The pulse is plotted on the same scale and normalized to $H_1 = 440$ MHz in the simulation. (**D**) Simulated final population of the $m_s = 0$ level as a function of pulse width for the same driving fields as in (B).

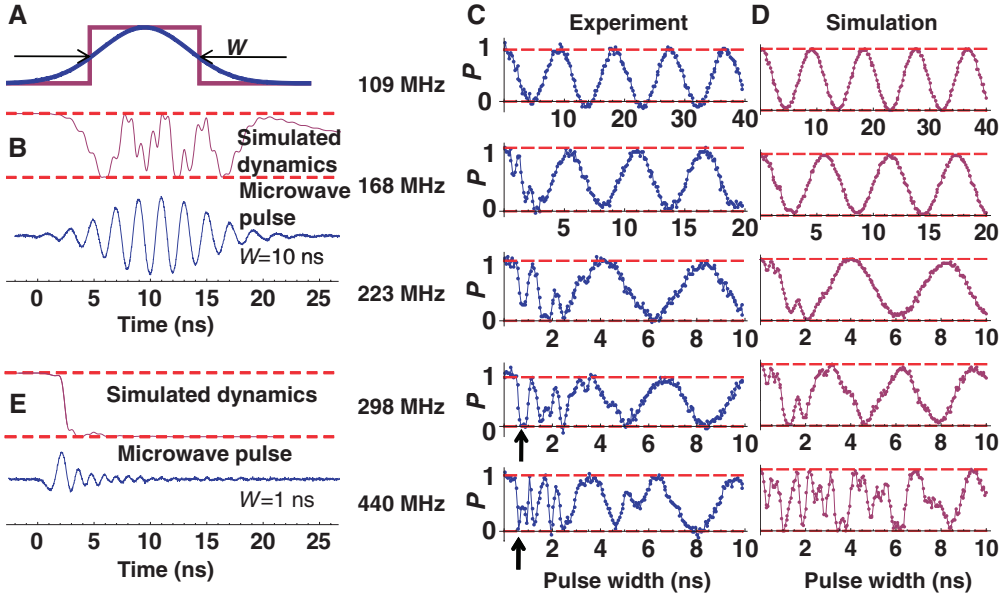

Fig. 3. (**A**) Comparison between the nominal envelope functions for square and Gaussian pulses. (**B**) Simulated time evolution of P for a $W = 10$ ns pulse with a peak $H_1 = 440$ MHz is plotted on the same scale. (**C**) Experimental Rabi oscillations using Gaussian pulses for five values of H_1. Each shows I_{PL} as a function of nominal pulse width, W. The dashed red lines show the values of I_{PL} level that correspond with $P = 1$ (upper) and 0 (lower). The two black arrows indicate points where the microwave pulse produces one spin flip in roughly half a Larmor precession cycle. (**D**) Simulated Rabi oscillations showing the final population of $m_s = 0$ as a function of W for the same values of H_1 as in (C). (**E**) Simulated time evolution of P for a $W = 1$ ns pulse with a peak $H_1 = 440$ MHz is plotted on the same scale.

agreement with the experiment and the previous simulation. This correspondence shows that, although transient effects exist, the experimental data reflect the true time evolution of the spin state. In addition, some differences between the simulation and the experiment are expected because the spin dynamics in this regime are sensitive to fine details of the pulse shape (*17*).

As a first step toward optimizing the strong-driving field, we engineered Gaussian-shaped pulses to mitigate pulse edge effects. The pulses were normalized so that the full-width at half maximum, W, is equal to the nominal width of a square pulse with the same area (Fig. 3A). Figure 3B shows the simulated time evolution of P during a $W = 10$ ns pulse with a peak $H_1 = 440$ MHz. The simulated dynamics have anharmonic features in the center of the pulse, with both sub-nanosecond rotations and stalling, but with more gradual spin rotation accumulating in the pulse edges.

We focused on the largest driving fields in the Gaussian pulse experiment, with smaller steps in H_1 (Fig. 3C), and plotted for comparison the simulations of final population (Fig. 3D). At $H_1 =$ 109 MHz, the Gaussian pulses recover sinusoidal Rabi oscillations compared with the steplike oscillations seen for the square pulses at the same driving field. As H_1 was increased, however, we saw the evolution of two separate regimes: subperiod duration pulses ($W < 2$ ns) and longer pulses. Subperiod pulses generated strongly anharmonic rotations, whereas longer pulses induced comparatively smooth Rabi oscillations with a rotation rate roughly linear in H_1. At $H_1 = 440$ MHz, there were some features of nonlinear rotations even for large W.

An important feature of these data are the reproducible spin flips from pulses with nominally sub-nanosecond values of W (arrows, Fig. 3C). The simulations confirm that, although the pulse has a nonresonant tail that is longer than a nanosecond because of ring-down in the amplifier, nearly all of the rotation occurs on sub-nanosecond time scales with little additional rotation from the tail. This can be seen in Fig. 3E, which shows that during the simulated evolution of P for a $W = 1$ ns pulse there is a spin flip in less than 1 ns. With additional experimental and theoretical effort, sub-Larmor cycle manipulation could be optimized for even faster quantum control of two-level systems.

As quantum information processing extends toward technology, advancements will be needed on several fronts. Understanding and controlling the dynamics in the strong-driving regime is a key step toward optimizing fast quantum control over two-level systems. When combined with rotations from Larmor precession, these results enable full quantum control at gigahertz rates. We have demonstrated that, although simple scaling of the driving field breaks down, strong driving offers opportunities to test advanced concepts of quantum control (*19*–*21*) and achieve faster state operation than expected from a driving field with conventional approaches. Moreover, by combining the millisecond coherence times in diamond (*25*) with the sub-nanosecond manipulation from strong-driving, more than a million coherent operations can be performed on a single NV center spin at room temperature.

References and Notes

1. R. Hanson, D. D. Awschalom, *Nature* **453**, 1043 (2008).
2. M. Hofheinz *et al.*, *Nature* **459**, 546 (2009).
3. L. DiCarlo *et al.*, *Nature* **460**, 240 (2009).
4. J. Berezovsky, M. H. Mikkelsen, N. G. Stoltz, L. A. Coldren, D. D. Awschalom, *Science* **320**, 349 (2008).
5. R. Hanson, L. P. Kouwenhoven, J. R. Petta, S. Tarucha, L. M. K. Vandersypen, *Rev. Mod. Phys.* **79**, 1217 (2007).
6. X. Xu *et al.*, *Nat. Phys.* **4**, 692 (2008).
7. J. Gorman, D. G. Hasko, D. A. Williams, *Phys. Rev. Lett.* **95**, 090502 (2005).
8. A. R. Stegner *et al.*, *Nat. Phys.* **2**, 835 (2006).
9. J. J. L. Morton *et al.*, *Nature* **455**, 1085 (2008).
10. F. Jelezko *et al.*, *Phys. Rev. Lett.* **93**, 130501 (2004).
11. L. Childress *et al.*, *Science* **314**, 281 (2006); published online 13 September 2006 (10.1126/science.1131871).
12. R. Hanson, V. V. Dobrovitski, A. E. Feiguin, O. Gywat, D. D. Awschalom, *Science* **320**, 352 (2008).
13. P. Neumann *et al.*, *Science* **320**, 1326 (2008); published online 13 March 2008 (10.1126/science.1155400).
14. M. A. Nielsen, I. L. Chuang, *Quantum Computations and Quantum Information* (Cambridge Univ. Press, Cambridge, 2002).
15. A. Abragam, *Principles of Nuclear Magnetism* (Oxford Univ. Press, Oxford, 1961).
16. S. Ashhab, J. R. Johansson, A. M. Zagoskin, F. Nori, *Phys. Rev. A* **75**, 063414 (2007).
17. J. K. Boyd, *J. Math. Phys.* **41**, 4330 (2000).
18. R. J. C. Spreeuw, N. J. van Druten, M. W. Beijersbergen, E. R. Eliel, J. P. Woerdman, *Phys. Rev. Lett.* **65**, 2642 (1990).
19. D. D'Alessandro, M. Dahleh, *IEEE Trans. Autom. Control* **46**, 866 (2001).
20. N. Khaneja, R. Brockett, S. J. Glaser, *Phys. Rev. A* **63**, 032308 (2001).
21. U. Boscain, P. Mason, *J. Math. Phys.* **47**, 062101 (2006).
22. F. Jelezko, T. Gaebel, I. Popa, A. Gruber, J. Wrachtrup, *Phys. Rev. Lett.* **92**, 076401 (2004).
23. L. J. Rogers, S. Armstrong, M. J. Sellars, N. B. Manson, *N. J. Phys.* **10**, 103024 (2008).
24. Materials and methods are available as supporting material on *Science* Online.
25. G. Balasubramanian *et al.*, *Nat. Mater.* **8**, 383 (2009).

26. We gratefully acknowledge support from the Air Force Office of Scientific Research, Army Research Office, and Defense Advanced Research Projects Agency. Work at the Ames Laboratory was supported by the U.S. Department of Energy Basic Energy Sciences under contract no. DE- AC02-07CH11358. We also thank R. Hanson and D. D'Alessandro for helpful discussions.

Supporting Online Material

www.sciencemag.org/cgi/content/full/1181193/DC1
Materials and Methods
SOM Text
Figs. S1 to S5
References

27 August 2009; accepted 28 October 2009
Published online 19 November 2009;
10.1126/science.1181193
Include this information when citing this paper.

Meteorite Kr in Earth's Mantle Suggests a Late Accretionary Source for the Atmosphere

Greg Holland,[1]* Martin Cassidy,[2] Chris J. Ballentine[1]

Noble gas isotopes are key tracers of both the origin of volatiles found within planets and the processes that control their eventual distribution between planetary interiors and atmospheres. Here, we report the discovery of primordial Kr in samples derived from Earth's mantle and show it to be consistent with a meteorite or fractionated solar nebula source. The high-precision Kr and Xe isotope data together suggest that Earth's interior acquired its volatiles from accretionary material similar to average carbonaceous chondrites and that the noble gases in Earth's atmosphere and oceans are dominantly derived from later volatile capture rather than impact degassing or outgassing of the solid Earth during its main accretionary stage.

There are many possible origins for planetary gases, but there is little evidence to identify whether or not the volatiles within our planet have the same accretionary origin as those that now form our oceans and atmosphere. After collapse of the solar nebula, planetesimals were formed from the dust within the first 0.1 to 1 million years (*1*). Although it took a further 100 million years of violent impacts between these planetary embryos before the terrestrial planets we see today remained, 60% of Earth's mass accumulated within the first 10 to 20 My (*1*, *2*). Solar nebula gas may have been present for as long as 10 My after nebula collapse was initiated (*3*) and contemporaneous with the terrestrial planet precursors. Indeed, gravitational capture of solar nebula gases by the early Earth (*4*) is used as a starting point for many noble gas and volatile accretionary models of both the terrestrial atmosphere and the interior (*5*, *6*). Alternatively, volatiles may have been carried to the early Earth by accreting dust, planetesimals (*7*), and cometary material (*8*). These sources would be composed of gases from implanted solar wind (*9*–*11*), adsorbed nebula gases (*12*), and minor amounts of presolar material.

[1]School of Earth, Atmospheric, and Environmental Sciences, University of Manchester, Oxford Road, Manchester M13 9PL, UK. [2]Department of Earth and Atmospheric Sciences, University of Houston, Houston, TX 77204–5007, USA.

*To whom correspondence should be addressed. E-mail: g.holland@manchester.ac.uk

Gigahertz Dynamics of a Strongly Driven Single Quantum Spin

G. D. Fuchs, V. V. Dobrovitski, D. M. Toyli, F. J. Heremans and D. D. Awschalom

Science **326** (5959), 1520-1522.
DOI: 10.1126/science.1181193originally published online November 19, 2009

Quick Spin Flips

Quantum computation holds the tantalizing promise of vastly improving the efficiency of traditional computers. Among the many solid-state candidates for storing and manipulating quantum information, nitrogen vacancy centers in diamond are especially attractive because they can be used at room temperature and stay operational for milliseconds at a time. To use this coherence time efficiently, it is important to achieve fast manipulation of the spins in the system. **Fuchs *et al.*** (p. 1520, published online 19 November; see the Perspective by **Gerardot and Öhberg**) used pulses of strong microwave magnetic field to probe the dynamics of single spins in a nitrogen vacancy center. In this "strong-driving" nonlinear regime, extremely quick spin flips of less than a nanosecond in duration were observed, offering the possibility that up to a million operations could be performed on a single spin during its coherence time.

Science (print ISSN 0036-8075; online ISSN 1095-9203) is published by the American Association for the Advancement of Science, 1200 New York Avenue NW, Washington, DC 20005.